

Strong-field non-sequential double ionization: wavelength dependence of ion momentum distributions for neon and argon

This article has been downloaded from IOPscience. Please scroll down to see the full text article.

2008 J. Phys. B: At. Mol. Opt. Phys. 41 031001

(<http://iopscience.iop.org/0953-4075/41/3/031001>)

View [the table of contents for this issue](#), or go to the [journal homepage](#) for more

Download details:

IP Address: 38.107.179.214

The article was downloaded on 21/02/2012 at 13:39

Please note that [terms and conditions apply](#).

FAST TRACK COMMUNICATION

Strong-field non-sequential double ionization: wavelength dependence of ion momentum distributions for neon and argon

A S Alnaser^{1,5}, D Comtois², A T Hasan¹, D M Villeneuve³, J-C Kieffer²
and I V Litvinyuk⁴

¹ Physics Department, American University of Sharjah, Sharjah, UAE

² INRS-Énergie, Matériaux et Télécommunications, 1650, boul. Lionel-Boulet, Varennes, Québec J3X 1S2, Canada

³ National Research Council of Canada, 100 Sussex Dr, Ottawa, Ontario, K1A 0R6, Canada

⁴ J R Macdonald Laboratory, Physics Department, Kansas State University, Manhattan, Kansas, 66506, USA

Received 1 December 2007, in final form 12 December 2007

Published 24 January 2008

Online at stacks.iop.org/JPhysB/41/031001

Abstract

Strong-field double ionization of atoms in a non-sequential regime produces longitudinal ion momentum distributions with a characteristic double-peak structure. At 800 nm laser wavelength in Ne²⁺ the structure is very pronounced with a well-resolved dip at zero momentum, while for Ar²⁺ the dip is very shallow, possibly indicating different mechanisms in the two atoms. We investigated the source of this difference by measuring longitudinal momentum distributions of Ne²⁺ and Ar²⁺ ions at different laser wavelengths (485, 800, 1313 and 2000 nm) and intensities. The shapes of the experimental momentum distributions for the two atoms exhibit strong dependence on laser wavelength: for both the dip becomes more pronounced at longer wavelengths. At 1300 nm the longitudinal momentum spectrum for Ar²⁺ is similar to that of Ne²⁺ at 800 nm. On the other hand, the Ne²⁺ spectrum measured at 485 nm has the same shape as that of Ar²⁺ at 800 nm. This observation indicates that the difference between Ne and Ar observed at 800 nm should not be attributed solely to differences in relative electron impact ionization and excitation cross-sections of the two atoms. It is, to a larger extent, due to the interplay between the ponderomotive energy of electron and the ionization potentials of the target atom.

Non-sequential double ionization (NSDI) is a dramatic enhancement in the production of doubly charged ions over the yields expected for simple sequential tunnelling mechanism. When NSDI was first observed in helium, it was originally suggested that the required two-electron interaction was due to the shake-off process [1]. Later, it became evident that the three-step electron re-scattering model proposed by Corkum [2] and Schaffer *et al* [3], in

addition to explaining the observed above-threshold ionization (ATI) and high harmonic generation (HHG) spectra, also well accounted for NSDI. The evidence in support of the re-scattering mechanism accumulated over the years to include experiments on ellipticity dependence of NSDI [4–6], ATI [7] and HHG [8, 9], ion recoil momentum distributions [10–13], correlated two-electron momentum distributions [14] and molecular clocks [15, 16]. It was also shown experimentally that shake-off/shake-up does not play an important role [17]. Following those developments, the three-step re-scattering

⁵ Author to whom any correspondence should be addressed.

model has become the basis for our understanding of strong-field phenomena in gas phase, serving as an important conceptual tool to guide further advances, particularly in the emerging field of atto-second physics.

According to the model an electron is first ionized by tunnelling through a potential barrier formed by the combined oscillating field of the laser and the Coulomb field of the ion core. Emerging in the continuum with near zero kinetic energy, an electron is accelerated by the laser field, causing it to quiver with the laser frequency and to drift with velocity dependent on the phase of the field at which ionization took place. Some of the electrons will return to the core and recombine or scatter elastically or inelastically. Recombination results in HHG, elastic scattering produces a high-energy plateau in ATI, inelastic scattering is responsible for NSDI. At the same time, newly formed singly and doubly charged ions also gain momentum from the field. After the laser pulse is over, the final recoil momentum of the ion will depend on the phase at which each ionization took place. For instance, singly charged ions are most likely to be produced at the peaks of the laser cycle and their longitudinal momentum distributions will have a maximum at zero momentum. The same would be true for doubly charged ions produced in the sequential regime, as both ionizations are likely to happen at the peak of the field oscillation. However, in the non-sequential regime the second ionization may happen when the first electron returns to the ion core with sufficient kinetic energy to directly knock out the second electron. Such an event is most likely to occur near zero of the field, and the resulting ion will gain substantial momentum along the field polarization direction. Thus, non-sequential ionization generally results in a double-peak longitudinal momentum distribution for doubly charged ions. In the case of multi-cycle pulses, or few-cycle pulses with unstable carrier-envelope phase, that distribution is symmetric with a minimum at zero momentum [18].

Additionally, the depth of that zero-momentum minimum appears to depend on a particular target. For instance, at 800 nm wavelength Ne^{2+} has a very pronounced minimum in its momentum distribution while for Ar^{2+} this minimum is barely present [11–13, 19]. Such a difference can be explained by postulating that in addition to the direct electron impact ionization pathway (responsible for the double-peak momentum distribution) the re-colliding electron also causes electronic excitation of the singly charged ion. The excited ion is then ionized at the maximum of the cycle later in the pulse, resulting in a momentum distribution peaked at zero. Those pathways can be disentangled by correlating the momentum of the ion with the emission directions of the two electrons. For direct impact ionization both electrons are most likely to go in the same direction, and ions associated with such events do indeed show pronounced minimum in their momentum distribution [20]. The relative branching ratio of the ionization and excitation pathways would determine the overall shape of the distribution. According to this explanation, in Ar the excitation pathway makes a much bigger contribution than in Ne, filling in the minimum. To understand the physical origin of that difference, de Jesus *et al* invoked different behaviour of field-free ionization and excitation cross-sections for Ne^+

and Ar^+ , pointing out that for Ar^+ excitation is more likely to occur, while in Ne^+ ionization has a larger cross-section [19].

Though such an explanation does look reasonable, it is not easy to substantiate with theoretical simulations. *Ab initio* calculations including detailed atomic structure are not yet feasible and various simplified models do not reproduce experimental momentum distributions well. Classical 3D trajectory simulations do show that there is a time delay between the first electron recollision and the ejection of the second electron [21]. The electron thermalization model [22] uses this time delay as an empirical parameter to fit the experimental ion momentum distributions for multiple (triple and higher) ionizations. In both cases the secondary electron ejection is delayed by about one quarter period and therefore can be interpreted as ionization from excited states at the peak of the field.

While the ion excitation and its relative yield in respect to the direct electron impact ionization do undoubtedly play a role in determining the shape of the longitudinal momentum distributions, that shape may also depend on a number of other factors, such as laser intensity (I), frequency (ω) and ionization potential of the target (I_p). The first two parameters together define the ponderomotive energy $U_p = I/4\omega^2$, the average energy of oscillating electrons. That energy, in turn, determines the maximum kinetic energy of re-colliding electrons ($3.17U_p$) and the maximum momentum an ion can gain from the laser pulse ($2z(U_p)^{1/2}$). The first quantity together with the second ionization potential (I_p^+) determines whether there is enough energy for direct electron impact ionization of the ion. The second quantity (ion's maximum momentum) determines how well the positive and negative momentum peaks are separated, and it clearly may affect the shape of the distribution as was experimentally demonstrated for helium [10, 19]. U_p also affects the width of the momentum distribution for ions produced by tunnelling at the peak of the field, where this width is given by $(3U_p I_p^{-3/2} I^{1/2})$ [23]. Depending on that width, the momentum peak at zero due to the excitation–ionization pathway may appear higher or lower, filling in or exposing the gap between the two direct impact ionization peaks⁶.

Additionally, the first ionization potential of the target determines the saturation intensity (I_{sat}), the largest intensity to which it can be exposed before getting depleted. Although saturation intensity may depend on the laser frequency and pulse duration, in tunnelling regime it can be well approximated by the barrier-suppression intensity, at which the potential barrier of the combined laser and Coulomb fields is lowered by more than the electron binding energy, $I_{\text{sat}} = (I_p^2/4z)^2$. Since for any target the effective laser intensity cannot exceed I_{sat} , it also determines the maximum possible value of U_p (and all other related parameters) at any given laser wavelength. For instance, argon has a much lower ionization potential (15.6 eV) than neon (21.6 eV). As a result, its first ionization saturates at lower intensity ($2.5 \times 10^{14} \text{ W cm}^{-2}$) than it does for Ne ($6 \times 10^{14} \text{ W cm}^{-2}$). So in any experiment with Ar raising the laser peak intensity beyond $3 \times 10^{14} \text{ W cm}^{-2}$ will not affect most of the relevant

⁶ Atomic units are used in the calculations throughout the communication.

parameters, causing only depletion of the neutrals earlier during the pulse⁷.

Perhaps even more importantly, the ion momentum distributions are also dependent on the specific ionization mechanism. Strictly speaking, the classical three-step model, and the conventional reasoning related to it, is valid only in the tunnelling regime, when the first ionization is most probable near the peak of the field and the resulting continuum electron starts with near-zero kinetic energy. Neither of those conditions is fulfilled in the multi-photon regime. In the multi-photon regime the first electron no longer has to be ionized at the peak of the field, or to return to the core with highest energy at the zero of the field, which would result in completely different momentum spectra. The transition from one regime to another is thought to occur when the Keldysh adiabaticity parameter ($\gamma = (I_p/2U_p)^{1/2}$) nears unity, with tunnelling being dominant at $\gamma \leq 1$. It is, however, well recognized that at intermediate values ($\gamma \approx 1$) the pure tunnelling picture is but a very crude model, and one needs to achieve $\gamma \leq 0.5$ to be safely in the tunnelling regime. For higher values of γ multi-photon effects may play an important role. For instance, at 800 nm wavelength the first ionization of argon cannot occur with adiabaticity parameter below 0.6, this minimum value being achieved with saturation intensity. For any experiment the effective value of γ will be even higher due to the focal volume effect, when most of the measured signals come from the lower intensity parts of the laser focus [24]. Not surprisingly, it was shown that multi-photon resonant effects (such as Freeman resonances [25]) are important in single ionization of argon even at 800 nm [26]. In comparison, for neon at 800 nm the Keldysh parameter can be as low as 0.4, allowing for the purer tunnelling ionization of this target.

It is hard to speculate on the relative role of various factors in determining the shape of longitudinal momentum distributions based on spectra measured for a single laser wavelength. To shed more light on this issue, here we present the results of wavelength-dependent studies, where we measured and compared longitudinal momentum distributions for doubly charged ions of argon and neon produced by intense laser pulses of different frequencies. The experiments were conducted at the Advanced Laser Light Source (ALLS) facility located in Varennes, Quebec. Laser pulses were generated by a high-power TOPAS optical parametric amplifier (OPA). The OPA was pumped by 800 nm, 70 fs, 7 mJ pulses generated by a Ti: sapphire system from Thales Lasers at 100 Hz repetition rate. An additional nonlinear mixing stage was used to generate the 483 nm wavelength. For all wavelengths the pulse duration was estimated to be 100–110 fs. After some attenuation by neutral density filters the laser pulses were focused by a spherical mirror (10 cm focal length) on a well-collimated supersonic jet of target atoms inside the uniform-electric-field ion imaging spectrometer. The resulting ions were collected and their full 3D momenta were

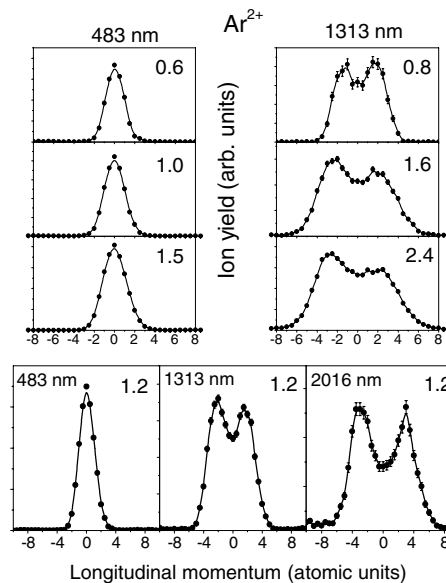


Figure 1. Longitudinal momentum distributions for Ar^{2+} ions measured at different wavelengths and peak intensities, as indicated for each spectrum. Intensities are given in the units of $10^{14} \text{ W cm}^{-2}$. The pulse duration is 100 fs. Asymmetry in the spectra is due to lower detection efficiency for ions ejected in the backward direction: a combination of smaller acceptance angle (inherent in the design of the ion spectrometer) and lower surviving factor for those ions.

measured by time- and position-sensitive delay-line anode detector at the end of the spectrometer. The supersonic jet propagation direction and the laser beam propagation direction were orthogonal to each other and both are orthogonal to the spectrometer axis. The laser electric field was polarized along the spectrometer axis. The laser peak intensities at the focus were derived either from a single ion momentum measurement with circular polarization (for 2020 nm, where a quarter waveplate was available) or from first principles based on measurements of focal spot sizes with an IR-sensitive CCD camera (all other wavelengths).

Figure 1 shows the experimental longitudinal momentum distributions measured for Ar^{2+} produced by different laser wavelengths and peak intensities. (The resolution in these spectra is ~ 0.5 au, basically determined by the TDC resolution.) At 483 nm for all intensities we observe a single-peak distribution centred at zero momentum. At this wavelength the maximum possible electron recollision energy for Ar is well below the second ionization potential (27.6 eV), making direct electron impact ionization impossible. Whether the Ar^{2+} ions produced at this wavelength are all generated by a sequential process or some other non-sequential mechanism is still operational remains an open question to be addressed in further studies. It must also be pointed out that at 483 nm the first ionization of a neutral Ar atom does not follow the tunnelling mechanism, so that the conventional three-step re-scattering model does not, strictly speaking, apply for this wavelength. At this frequency the laser electric field completely suppresses the potential barrier to ionization before the Keldysh adiabaticity parameter γ ever gets below unity, a value typically associated with transition-to-tunnelling

⁷ While de Jesus *et al* [12] try to scale their 800 nm spectra according to assumed maximum energy of recolliding electrons (3.17 times ponderomotive energy), all their Ar spectra were acquired near or above the saturation intensity, so that the effective electron recollision energies were more or less the same for all Ar spectra presented in that paper.

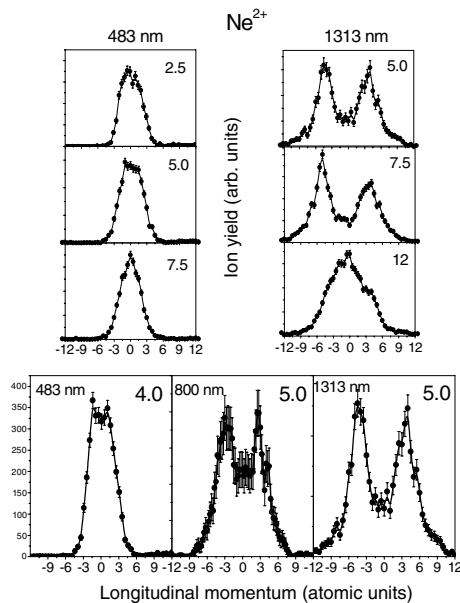


Figure 2. Longitudinal momentum distributions for Ne^{2+} ions measured at different wavelengths and peak intensities. Intensities are given in the units of $10^{14} \text{ W cm}^{-2}$. The pulse duration for 483 nm and 1313 nm is 100 fs. The pulse duration for 800 nm is 70 fs.

ionization. As a result, increasing intensity switches ionization mechanism from multi-photon directly to over-the-barrier, skipping over the tunnelling. Therefore, in these conditions conventional reasoning based on the usual re-scattering model should not be relied on for an insight on possible momentum distributions.

For wavelengths longer than 800 nm and sufficiently high intensities tunnelling is certainly a dominant ionization mechanism. Here, the three-step model gains its heuristic usefulness and comparisons can be made with much better validity. At 1313 nm Ar^{2+} momentum distributions start to exhibit a pronounced dip and have a shape similar to that of Ne^{2+} at 800 nm. One can also see that separation between the peaks increases with intensity. Going to the even longer wavelength of 2020 nm continues this trend—the dip at zero momentum becomes even more pronounced.

It is interesting to compare Ar momentum distributions to those measured for Ne shown in figure 2. Due to its much higher first ionization potential in Ne, unlike in Ar, it is possible to produce recolliding electrons with energies near the second ionization potential (40.96 eV) even at 483 nm wavelength. It is also possible to achieve values of $\gamma \leq 1$ without complete barrier suppression, allowing tunnelling ionization. This is evident by a double-peak shape of momentum distribution seen at appropriate intensity. Both decreasing and increasing intensity reduce distribution to a single-peak shape. Reducing the intensity affects the distribution in two ways: (i) ponderomotive and electron recollision energies are lower with the latter getting below the second ionization potential, and (ii) first ionization becomes more multi-photon and less tunnelling in character. Both effects would result in loss of the double-peak structure. However, as the intensity increases

sequential double ionization takes over with the same effect on momentum distribution. It is worth noting that when the dip is observed at 483 nm for Ne^{2+} , the distribution looks remarkably similar to that of Ar at 800 nm [19]. Also in Ne, similar to Ar, going to longer 1313 nm wavelength increases the dip in comparison to its 800 nm spectra. At sufficiently high intensity the sequential mechanism starts to dominate, resulting in a single-peak distribution.

The clearly universal feature of momentum spectra for both targets is that the dip at zero momentum is very prominent at sufficiently long wavelengths, becomes less so as wavelengths are decreasing to the point of complete disappearance for all intensities at some critically high frequency. Probably, several different factors do contribute to this universal wavelength dependence. For instance, it can be readily explained within the purely tunnelling model simply by pointing out that the width of the excitation–ionization band centred at zero momentum will strongly depend on laser frequency: $\Delta p = 3U_p I^{1/2} (I_p^{+*})^{-3/2} = 3(I/I_p^{+*})^{3/2} (4\omega^2)^{-1}$, where I_p^{+*} is the ionization potential of the collisionally excited state of the ion involved in this pathway [23]. For lower frequencies this width strongly increases, effectively lowering the height of the band and exposing the dip. But transition from tunnelling to multi-photon ionization mechanism at shorter wavelengths must also play its role.

Though the progression of momentum spectra with laser wavelength is itself universal, for neon this transition takes place at higher laser frequencies than for argon. Even with 483 nm pulses one can observe the dip in Ne^{2+} spectra while for Ar 800 nm is already near the end of this range. Most of this difference can be accounted for by different values of the first and second ionization potentials of the two targets, without having to refer to more specific differences of their atomic structure. Thus to see a dip at zero momentum one must remove the first electron through tunnelling ionization and make it re-collide with enough energy to overcome the second ionization potential. While the parameters of neon make this possible even with 483 nm laser pulses, for argon even 800 nm is already near the limit.

Another intriguing observation is that the dependence of momentum spectra of Ne and Ar on laser wavelength seems to exhibit scaling similarity with scaling parameter $\alpha = (I_p^3/\omega^2)$, where I_p is the ionization potential and ω is the laser frequency. For instance, momentum distribution for Ne at $\lambda = 483$ nm ($\alpha = 55$, using atomic units) is similar to that of Ar at $\lambda = 800$ nm ($\alpha = 60$). Increasing the wavelength to 1313 nm for Ar makes $\alpha = 140$, which is close to that of Ne at $\lambda = 800$ nm ($\alpha = 150$), and the corresponding momentum spectra are also remarkably similar. Moreover, Ar spectra at 2020 nm ($\alpha = 350$) resemble those of Ne at 1313 nm ($\alpha = 400$). It is also interesting that this scaling parameter α is simply inversely proportional to the square of Keldysh parameter γ evaluated at barrier suppression intensity $(I_p^2/4z)^2$ for each target: $\gamma^{-2} = (I_p/2U_p)^{-1} = (64I_p\omega^2/2I_p^4)^{-1} = (I_p^3/32\omega^2)$. That is the lowest possible value Keldysh parameter can reach for a given target at a given wavelength before the potential barrier is completely suppressed. Whether this apparent scaling rule reflects some more fundamental inherent universality of

underlying physics or is a mere coincidence unique to the Ar–Ne pair is a question worthy of further investigation.

In conclusion, we measured longitudinal momentum distributions for doubly charged ions of argon and neon, produced by intense laser pulses of different wavelengths. The measured momentum spectra of both targets exhibit the same wavelength dependence, progressing from pronounced double-peak structure at long wavelengths to a lack of structure at short wavelengths. We hesitate to attribute this behaviour to a single dominating cause, since several different factors are likely to play a role. We do attribute the difference between argon and neon mainly to their differing ionization potentials, though more specific details of their atomic structure, such as relative ionization/excitation cross-sections and particular excited states of the ions, may also play a role. More complete understanding of the underlying physics will remain elusive until realistic theoretical calculations taking into account the electronic structure of atoms and ions can be performed and compared with more detailed wavelength-dependent experiments.

Acknowledgments

We are grateful to Drs Lew Cocke, Xiao-Min Tong and Artem Rudenko for helpful discussions and suggestions. We gratefully acknowledge the ALLS laboratory's technical staff for their assistance throughout the course of this work. IVL acknowledges support from Chemical Sciences, Geosciences and Biosciences Division, Office of Basic Energy Sciences, Office of Science, US Department of Energy. ASA acknowledges support from FRG grant from the American University of Sharjah, UAE.

References

- [1] Fittinghoff D N *et al* 1992 *Phys. Rev. Lett.* **69** 2642
- [2] Corkum P B 1993 *Phys. Rev. Lett.* **71** 1994
- [3] Schafer K J, Young B, DiMauro L F and Kulander K C 1993 *Phys. Rev. Lett.* **70** 1599
- [4] Fittinghoff D N *et al* 1993 *Phys. Rev. A* **49** 2174
- [5] Walker B *et al* 1993 *Phys. Rev. A* **48** 894
- [6] Kondo K *et al* 1993 *Phys. Rev. A* **48** 2531
- [7] Paulus G G *et al* 2000 *Phys. Rev. Lett.* **84** 3791
- [8] Budil K S *et al* 1993 *Phys. Rev. A* **48** R3437
- [9] Mercer I *et al* 1996 *Phys. Rev. Lett.* **77** 1731
- [10] Weber Th *et al* 2000 *Phys. Rev. Lett.* **84** 443
- [11] Weber Th *et al* 2000 *J. Phys. B: At. Mol. Opt. Phys.* **33** L127
- [12] Moshhammer R *et al* 2000 *Phys. Rev. Lett.* **84** 447
- [13] Moshhammer R *et al* 2003 *J. Phys. B: At. Mol. Opt. Phys.* **36** L113
- [14] Weber Th *et al* 2000 *Nature* **405** 658
- [15] Niikura H *et al* 2002 *Nature* **417** 917
- [16] Niikura H *et al* 2003 *Nature* **421** 826
- [17] Litvinyuk I V *et al* 2005 *Phys. Rev. Lett.* **94** 033003
- [18] Liu X *et al* 2004 *Phys. Rev. Lett.* **93** 263001
- [19] de Jesus V L B *et al* 2004 *J. Phys. B: At. Mol. Opt. Phys.* **37** L161
- [20] Feuerstein B *et al* 2001 *Phys. Rev. Lett.* **87** 043003
- [21] Haan S L, Breen L, Karim A and Eberly J H 2006 *Phys. Rev. Lett.* **97** 103008
- [22] Liu X, Figueira de Morisson Faria C, Becker W and Corkum P B 2006 *J. Phys. B: At. Mol. Opt. Phys.* **39** L305
- [23] Delone N B and Krainov V P 1998 *Phys.-Usp.* **41** 469
- [24] Morishita T, Chen Z, Watanabe S and Lin C D 2007 *Phys. Rev. A* **75** 023407
- [25] Freeman R R, Bucksbaum P H, Milchberg M, Darack S, Schumacher D and Geusic M E 1987 *Phys. Rev. Lett.* **59** 1092
- [26] Maharjan C M, Alnaser A S, Litvinyuk I, Ranitovic P and Cocke C L 2006 *J. Phys. B: At. Mol. Opt. Phys.* **39** 1955